INTERNATIONAL ATOMIC ENERGY AGENCY
UNITED NATIONS EDUCATIONAL, SCIENTIFIC AND CULTURAL ORGANIZATION

INTERNATIONAL CENTRE FOR THEORETICAL PHYSICS
34100 TRIESTE (ITALY) - P.O.B. 586 - MIRAMARE - STRADA COSTIERA 11 - TELEPHONE: 2240-1
CABLE: CENTRATOM - TELEX 460392-I

H4.SMR/285 - 16

WINTER COLLEGE ON
LASER PHYSICS: SEMICONDUCTOR LASERS
AND INTEGRATED OPTICS

(22 February - 11 March 1988)

PHOTODETECTORS FOR INTEGRATED OPTICS

H. Melchior
Swiss Federal Institute of Technology
Zürich, Switzerland

PHOTODETECTORS FOR INTEGRATED OPTICS

H.Melchior

Swiss Federal Intitute of Technology
CH 8093 Zürich, Switzerland

Abstract:
Integrated optics for signal processing, optical communication and image detection appears interesting not only at wavelengths throughout the visible part of the spectrum but at wavelengths in the infrared as well. While it is true that present dispositions of integrated optics rarely include fully integrated detectors, hybrid and monolithic integration of optics and detectors will become more prevalent as optoelectronic integration advances in the future. Keeping with the present state of the art this tutorial thus presents an overview mostly over nonintegrated photodetectors for visible and near infrared wavelengths including the wavelengths of 0.8 and 1.2 to 1.6µm which are of major interest for fiber optical communication. After briefly mentioning the role of thermal detectors, this presentation concentrates on photodiodes and avalanche photodiodes. Design and selection criteria for the efficient detection of weak light signals will be mentioned including quantum efficiency and responsivity of photodetectors and signal-to-noise rations and error rates of optical receivers.

I. Introduction

Integrated optics is of interest for the miniaturization of existing optics concepts and for the extension and realization of new functions in optical signal precessing, optical-fiber lightwave communication and for the detection and processing of infrared radiation. Forseable applications entice the entire wavelengths range throughout the visible to 0.8 and from 1.2 to 1.6 micrometers where major interest in fiber-optical communication centers and to longer wavelengths in the infrared.

Photodetectors /1/ for these wavelengths include thermal detector-types, like bolometers for monitoring and calibration purposes and pyroelectric detectors for convenient detection of high speed signals of high intensity /2/. These detectors respond to the rate at which energy is absorbed. The best and most commonly used detectors for the sensing of radiation throughout parts of the visible and the nearer infrared range of the spectrum are all photodetectors based on the photoelectric effect /1/. In these detectors absorbed photons are, as illustrated in Fig.1, able to excite electrons from lower to higher energy levels, thereby giving rise to the flow of photocurrent through the detector.

These photodetectors respond to the rate at which photons are absorbed. Such photodetectors for visible and near infrared wavelengths use photoconductive materials in which photons are able to excite electrons directely from the valence (V) into the conduction band (C). Photons are then absorbed and able to excite carriers as long as their energy hν is higher than the bandgap-energy ΔE of the respective photodetector. Photondetectors based on band-to-band excitation in a semiconducting material thus possess a detection limit towards long wavelengths (λ) /1-6/:

$$\lambda \leq \lambda_{max}\ [\mu m] \leq \frac{1.24}{\Delta E[eV]}. \qquad (1)$$

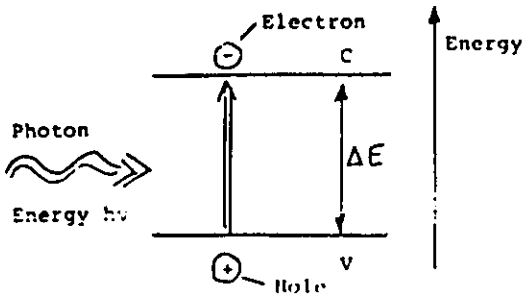

Fig.1 Photoeffect (Einstein 1905): Photon with evergy hν (h = Plancks constant, ν = optical frequency) is absorbed and excites electron-hole pair in photodetector.

Silicon (ΔE = 1.12ev) is the most commonly used photodetector material for visible and near infrared wavelengths around 0.8 and 0.9μm where AlGaAs semiconductor lasers and light emission diodes operate. Its technology is will known. It allows detector optimization, array fabrication and integration with electronic receivers. Extension of the response towards longer wavelengths between 1.2 and 1.6 micrometers, the major wavelengths of present interest in fiber-optical communication, needs other detector materials. Germanium (ΔE = 0.66eV) extends the response to about 1.5μm /8,9/. Detectors in III-V compounds like InGaAs and InGaAsP on InP have undergone intensive development in recent years /10-17/ with excellent detectors and detector-amplifier combinations /18-21/ becoming available.

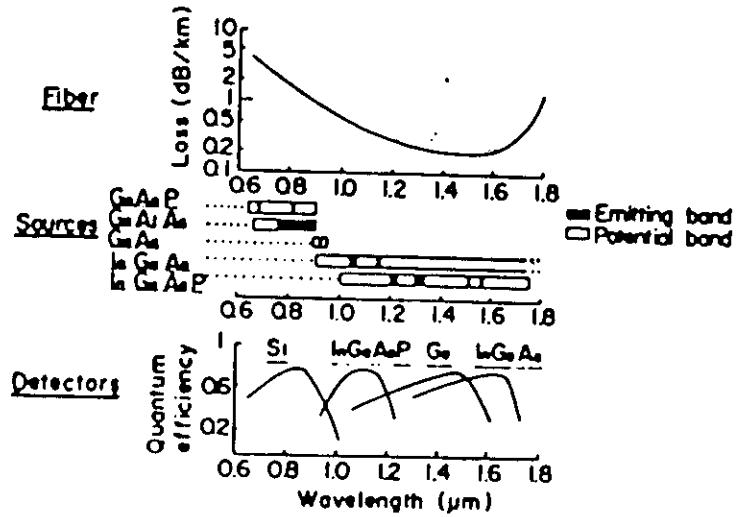

Fig.2 Fiber-optical communication in 1.2-1.6μm range. Low-loss wavelength region of fiber, emission wavelengths of semiconductor light sources and wavelength responses of semiconductor photodetectors (after /7/).

Integrated optics has advanced to the stage, where waveguides, modulators and switches can be combined in monolithic form. Inclusion of semiconductor light sources and detectors has up to now in essence not passed the stage of hybrid integration. As far as the monolithic integration of detectors and optical waveguides is concerned only a few attempts and demonstrations have been reported. A case in point is the integrated optics detector with waveguide conceived by D.B.Ostrowsky et.al. /22/. As shown schematically in Fig.3, this detector combines a silicon photodiode with an optical waveguide in SiO_2.

At present virtually all integrated optics arrangements rely on separated, single, well designed and optimized detectors, arrays, or detector-receiver combinations.

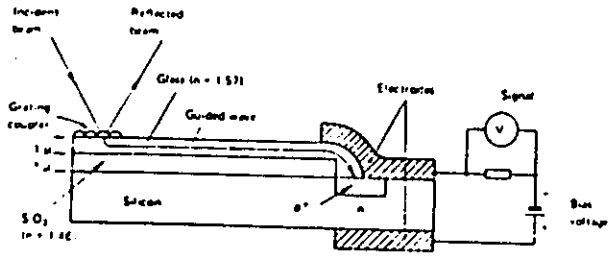

Schematic of a hybrid integrated optics detector in silicon

Fig. 3 Integrated optics detector with SiO_2-waveguide and Silicon photodiode (after /22/).

In keeping with this present state of the art, this presentation will concentrate on single and optical receivers with well optimized response at visible and near infrared wavelenghts. Reverse biased photodiodes without or with internal current gain, i.e., avalanche carrier multiplication are the most suitable detectors for these wavelengths /1,3-8,23/. They exhibit high responsivity, low leakage currents, high speed of response and good sensitivity to weak light signals /1/.

In the following, the principle of operation and behaviour of photodiodes will be described. It will be pointed out how these detectors are combined with low noise electronic receivers to detect weak optical signals with good signal-to-noise ratio or low error rates. Attention will be drawn to the advantages and the increase in sensitivity that is possible with avalanche-photodiode-receivers. It is then pointed out that the infrared sensitive avalanche photodiodes do not yet reach the sensitivities of the best silicon avalanche photodiodes. This has lead to the search for improved avalanche multiplication structures /24,25/ and to the investigation of optical heterodyne detection techniques /1,26,27/. The simpler technology

of photodiodes and the lack of low noise avalanche structures has for the 1.2 to 1.6µm range lead to the development of monolithically integrated low noise InGaAs-photodiode-field effect transistor receivers with good sensitivity to weak infrared signals.

II. Photodiodes

The photodetector type most commonly used in integrated optics and fiber-optical communication is the photodiode which has as its essential feature a reverse biased p-n junction in a semiconductor capable of absorbing the incident radiation /1,6,24/. The operation of a reverse biased photodiode is illustrated in Fig.4.

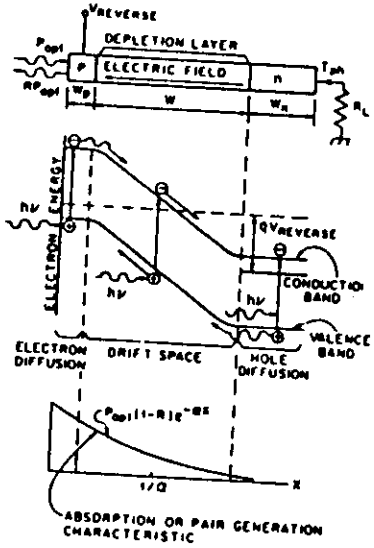

Fig.4 Operation of solid state photodiode. Cross-sectional view of p-i-n diode and energy band diagram under reverse bias conditions is shown together with optical absorption and pair generation characteristic.

Electrons and holes generated by the absorbed photons are separated under the influence of the built-in and applied bias field and drift in opposite directions thereby inducing a current in the external circuit which is then amplified and processed.

The p-i-n photodiode, as normally fabricated, consists of a lightly doped p or n type layer (the i-layer) sandwitched between two learity doped p and n regions, Fig.5.

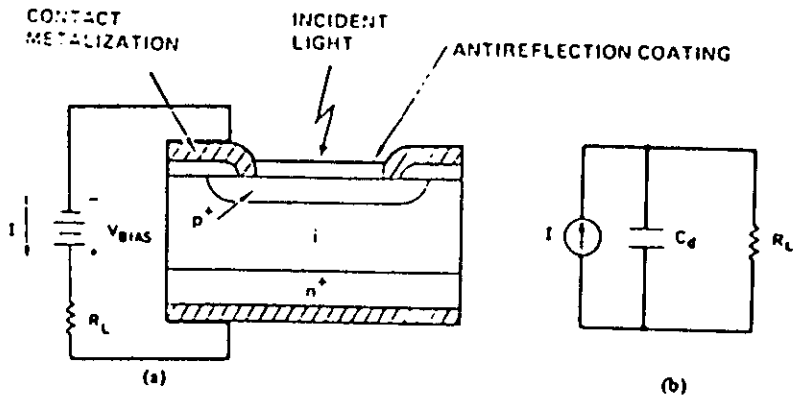

Fig.5a) Schematic view of silicon p-i-n photodiode.
b) Equivalent circuit of device without leakages and series resistances.

A reverse bias is applied which depletes the i region. Efficient conversion of the incoming photons into photoelectrons require the incident photons in their majority to be absorbed within the high field i region of the device. In operation the photodiode looks like a current source with the photogenerated current given by

$$I_{ph} = \eta e \frac{P_{opt}}{h\nu} \qquad (2)$$

where $h\nu$ is the photon energy, e the electron charge and P_{opt} is the optical power incident on the detector. The quantity η is the quantum efficiency of the detector and represents the fraction of the incident photons producing electron-hole pairs that are collected as photocurrent. C_d is the capacitance seen by the photocurrent generator while driving the load $R_L \cdot C_d$ comprises the junction capacitance of the photodiode, the capacitance of the mount and the input of the load circuit.

The p-i-n construction allows tayloring of optimization of quantum efficiency and speed of response. This is of special importance for Silicon whose absorption constant varies gradually with wavelengths. To absorb all the light within the high field region ($\alpha w \geq 2$) long wavelength sensitive diodes need wide intrinsic w regions /1/.

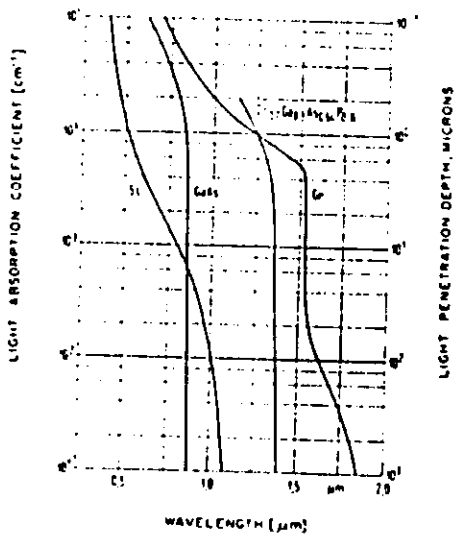

Fig.6 Optical absorption coefficients of major photodetector materials /1,4/.

Silicon photodiodes for blue and UV light possess high field regions that extend close to the surface towards the incident radiation /1/. Large efficiency (>80%) arround 6000 Å and high speed of response as short as 40ps can be obtained from Si p-i-n diodes with 2-3µm wide high field regions /24/. To insure high quantum efficiencies (>80%) at GaAs-laser wavelengths between 0.8 and 0.9µm the Si p-i-n diode need high field regions that are as wide as 20 to 40µm. Transit-times of the carriers through these wide drift regions will then however limit the speed of response to around one nanosecond. The gradual drop-off of the absorption constant of silicon with wavelength thus leads to an undesired trade-off between efficiency and speed of response.

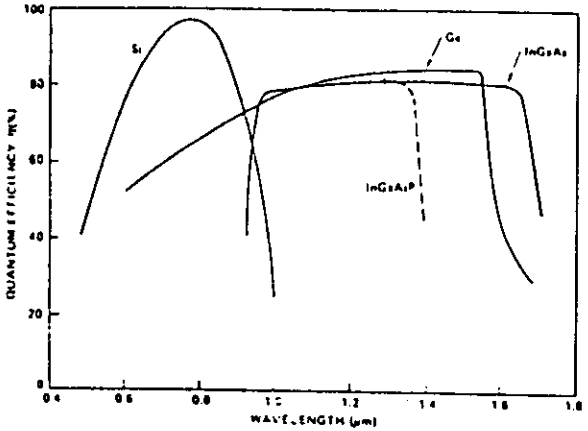

Fig.7 Spectral response of typical photodiodes.

Better response and high speeds are achieved as illustrated in Fig.7 with p-i-n diodes made from germanium /8,9/ or III-V materials such as InGaAs and InGaAsP /10-17/. In an interesting development /28/, HgCdTe-diodes have been realized with response in the 1.3-1.5µm region and towards longer wavelengths in the infrared.

Silicon photodiodes are in a state of relative maturity. Large and small area devices are available in single units, linear /35/ and two-dimensional arrays /29,30/. Photodiodes for use in infrared optics and fiber optical communication are usually small in size with diametres of the light sensitive area between 20 and 200µm. Their junction capacitances can be below 1pF and the dark currents of order 1nA. Highest speeds approaching 100GHz are achieved with miniaturized devices of a few µm in dimension embedded in microwave packages /31/.

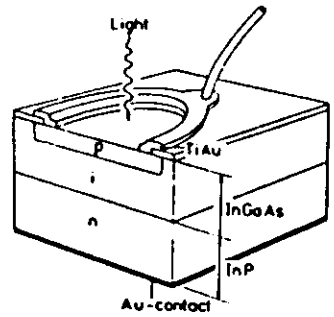

Fig.8 InGaAs p-i-n photodiode for integrated optics and fiber-optical communication in the 1-1.6µm wavelength range /10-17/.

The construction and cross-sectional view of a InGaAs p-i-n photodiode for the 1 to 1.6µm range is illustrated in Fig.8.

The signals emerging from photodiodes are usually quite small. A light signal of 100nW creates a photocurrent of less than 100nA. For convenient processing photodiode signals thus need to be amplified in low noise receivers.

III. Optical Receivers

An optical receiver detects optical signals and amplifies it then for use in electronic signal processing. Usually an optical receiver consists of a photodetector and an electronic amplifier of sufficient bandwidth and low noise to pass and amplify the weak signals emerging from the photodetector /1-7/.

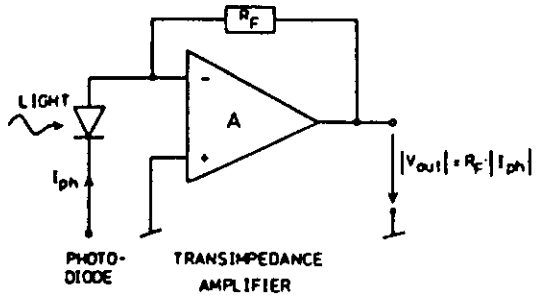

Fig.9 Optical receiver with transimpedance amplifier.

Two types of amplifiers are in common use, one is a low noise amplifier with a high impedance input /32,23/, the other is the so called transimpedance amplifier /33,23/. In the transimpedance amplifier the photocurrent is forced through the feedback resistor R_F to generate an output voltage

$$V_{out} = -R_F \cdot I_{ph}, \qquad (3)$$

that is proportional to the photocurrent I_{ph}. A variety of amplifier circuits have become known /23,32-35/ with good signal amplification, large dynamic range and low noise in bandwidths of up to tens and hundreds of MHz, with the fastest ones extending into the GHz range.

If sufficiently large light intensities are available the major performance criteria for an optical receiver are good responsivity (A/W) and quantum efficiency of the photodiode at the wavelength of operation and sufficient bandwidth of the receiver electronics to pass the photogenerated signal.

If weak light signals are to be detected, then minimization of noise and interference pickups becomes a major requirement for the receiver. Receiver noise includes contributions from the electronic amplifier and shot noise from the total detector current.

The light detection process in a photodiode consists of the absorption of photons which produce electron-hole pairs, each of which induces a current in the external circuit. Since the arrival times of the photons are random and usually (in the absence of strongly coherent fluctuations) /36-18/ characterized by Poisson statistics /2,36/, the current produced in a given time interval is also random. The fluctuations in the current are referred to as shot noise. For a photocurrent I_{ph}, the fluctuations in the current are characterized by a mean square noise spectral density

$$\frac{\langle i_{Det}^2 \rangle}{\Delta f} = 2e\, I_{ph}, \qquad (4)$$

where Δf is an electrical frequency band of the receiver. This noise is associated with the incident radiation and represents the fundamental limitation (quantum limit) of the detection process /1-6/. In an actual photodiode, nonnegli-

gible dark and background radiation induced currents might add to the shot noise /1,6/.

For analog signal transmission the goal is to detect the weakest possible light signals while still maintaining an adequate signal-to-noise ratio (SNR) at the output of the optical receiver /1-6/.

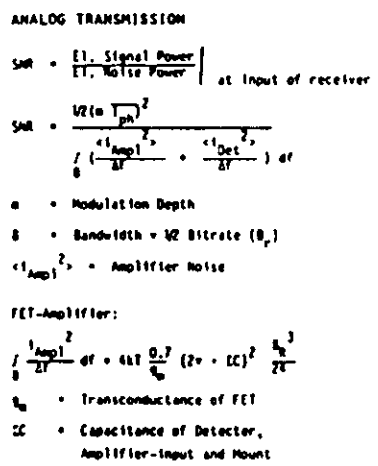

Fig.10 Signal-to-noise ratio of photodiode-receiver.

The SNR is commonly defined as the ratio of the electrical signal to the noise power and reffered to the input of the receiver.

When weak light signals have to be detected, then in almost all practical cases the sensitivity (SNR) is limited by amplifier noise:

$$\langle P_{opt,min}\rangle = \frac{h\nu}{\eta e}\cdot\frac{2}{m}\cdot(SNR)\cdot B\cdot\frac{\langle i_{Det}^2\rangle}{\Delta f} \qquad (5)$$

within the bandwidth B of the receiver /1-6/.

While SNR's for digital systems are of order 20dB, even when error rates have to be maintained below 10^{-9}, analog signal transmission of sound and video signals can require SNR's exceeding 50dB's.

To detect weak light signals it would thus help to employ either photodetectors with built-in low noise gain such as avalanche photodiodes or a photodetection process such as optical heterodyning that overcomes the noise limitations of the receiver /1/. While avalanche photodiodes are quite practical and will thus be treated in the next section, optical heterodyne detection at visible and near infrared wavelengths is at an early stage of exploration. Interested readers are referred to the literature /26,27,7,1/.

Low amplifier noise requires careful design of the receiver. Capacitances of the photodetector, mount and receiver input have to be minimized. This is illustrated in Fig.10 where the noise of a field effect transistor amplifier is detailed. Besides chosing a FET with high transconductance g_m it is of utmost importance to keep the capacitances ΣC at the input of the receiver at their lowest possible values. In discrete and hybrid integrated receivers /35/ these capacitances can hardly be lowered under a few pF, even if the detector capacitances are considerably lower. As will be shown lateron in Fig.22, this limits the sensitivity and the minimal detectable power of discrete photodiode receivers for digital signal reception in the 50 to 500MHz region to -40 and -30dBm.

Photodetectors with internal current gain bring advantages especially at wavelengths where the well developed silicon avalanche photodiodes operate.

Monolithic integration of photodetector and low noise receiver is another avenue which is actively pursued to achieve higher sensitivities /9.39-/. Such integration has already advanced from the stage of photodetector-field effect transistor integration /19/ to the integration of entire receivers /19,20,39-41/.

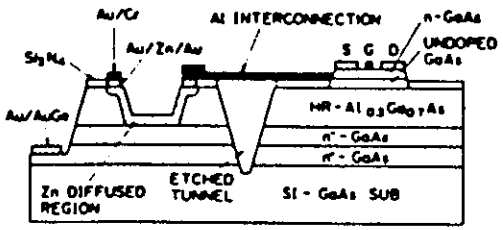

Fig.11 Structure of AlGaAs-p-i-n-FET receiver.

Since full integration eliminates major points of the mounting and stray capacitances, receiver sensitivities improve considerably, by several dBs. As an example, receiver front-end modules using GaAs p-i-n-FET's have been successfully demonstrated in combination with integrated GaAs amplifiers, showing the capability of receiving digital signals at 400Mbit/sec and 0.85um wavelength /40,41/.

IV. Avalanche Photodiodes

Compared to simple photodiodes avalanche photodiodes (APD's) possess internal current gain which helps to overcome the noise limits of the receiver so as to achieve higher sensitivities /1,8/.

Avalanche photodiodes are especially constructed photodiodes which can be operated at high reverse bias voltages where avalanche carrier multiplication takes place. At high electric fields in excess of 10^5V/cm, electrons and holes which drift through the junction can pick up sufficient energy to excite new electron-hole pairs through impact ionization /1,3,4,42,43/.

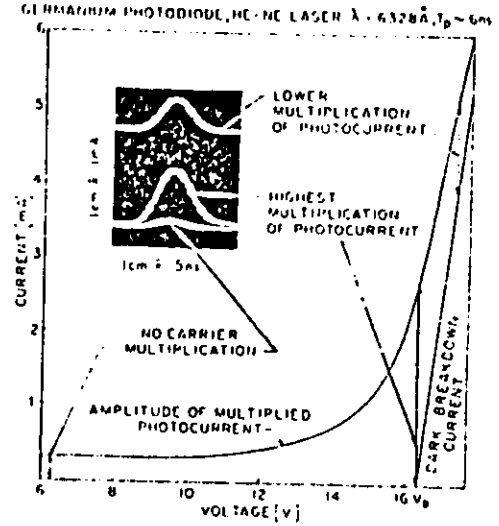

Fig.12 Pulse response and carrier multiplication of germanium avalanche photodiode /8/.

The operation of an avalanche photodiode is illustrated in Fig.12. Photoresponse and dark current characteristics of a germanium avalanche photodiode are shown as it is excited with 0.5ns pulses from a pulse locked helium neon laser /8/. At low reverse bias voltages, where no carrier multiplication takes place, the diode operates as a regular photodiode. As the reverse bias is increased, carrier multiplication

through impact ionization sets in, as indicated by an increase in the current pulse. The highest pulse amplitude and maximum photocurrent multiplication is reached, when the diode is biased close to the breakdown voltage V_B. At higher voltages, a self-sustained dark-breakdown current renders the diode less sensitive to photon-excited carriers.

In an avalanche photodiode the photo-generated electron-hole pairs generate additional carriers, resulting in an output current that is larger than the primary photocurrent given by eq.2. The equivalent circuit of Fig.5b) may be used for the APD with the value of the current now given by

$$I = \langle M \rangle I_{ph} = \langle M \rangle \frac{\eta e}{h\nu} P_{opt} \qquad (6)$$

where <M> is the average carrier multiplication factor. The avalanche gain depends on the photodetector material, device design and on the bias conditions and the temperature of operation.

The avalanche gain process is actually a statistical process /44/ in which each primary carrier produces a random number M of secondary carriers with a mean value <M>. The random nature of the avalanche gain introduces noise into the photocurrent multiplication process. As compared to a photodiode, the mean square noise spectral density of the multiplied photocurrent increases to

$$\frac{\langle i_{Det}^2 \rangle}{\Delta f} = 2eI_{ph} \cdot \langle M \rangle^2 \cdot F(\langle M \rangle), \qquad (7)$$

where F(<M>) is referred to as the excess noise factor /44/.

In an ideal multiplier the excess noise factor would be unity.

In an actual photodetector the excess noise factor depends on the detector material, the shape of the electric field profile within the device and on whether the avalanche is initiated by electrons and holes /1,24,44/. F(<M>) will be smallest when only one type of carriers (electrons or holes) produces ionizing collisions and the avalanche is initiated by this type of carrier. After McIntyre /44/ the excess noise factor increases as

$$F(\langle M \rangle) = k\langle M \rangle + (2 - \frac{1}{\langle M \rangle})(1-k) \qquad (8)$$

when the avalanche is initiated by the more strongly ionizing carrier.

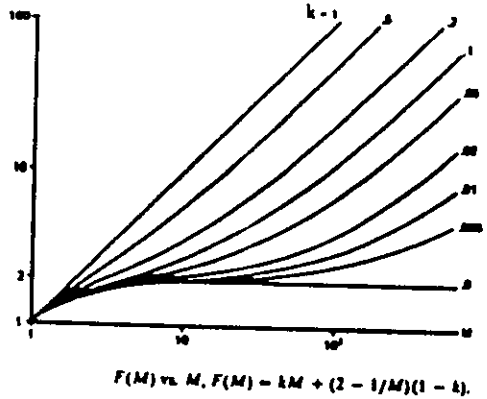

Fig.13 Excess noise factor F(M) of avalanche carrier multiplication process as a function of average carrier multiplication M and ratio k of the smaller to the larger ionization coefficient and where the most ionizing type of carriers initiates the avalanche /44/.

In this equation, the factor k denotes the ratio of the weaker to the stronger ionization coefficient. The best performance is achieved when k is small and the avalanche is initiated with the strongly ionizing type of carriers.

Ionization rates of electrons and holes for the most common avalanche photodetector materials are shown in Fig.14.

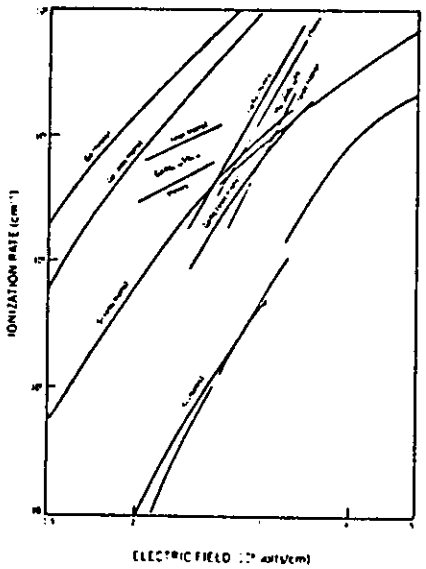

Fig.14 Ionization rates of electrons and holes in silicon, germanium and III-V photodetector materials /1,24,42,43/.

The largest differences between the ionization rates of holes and electrons are found in silicon. Silicon is thus the best material for avalanche photodiodes. It is an electron multiplier that exhibits k values as low as 0.02, especially at low fields.

To take full advantage of the possibilities offered by silicon for an almost fluctuation-free and high-speed photoelectron multiplication /44,45/, silicon avalanche photodiodes have to be constructed in a special way. The n^+-p-π-p^+ reach-through structures /46/ are the best /47-49/.

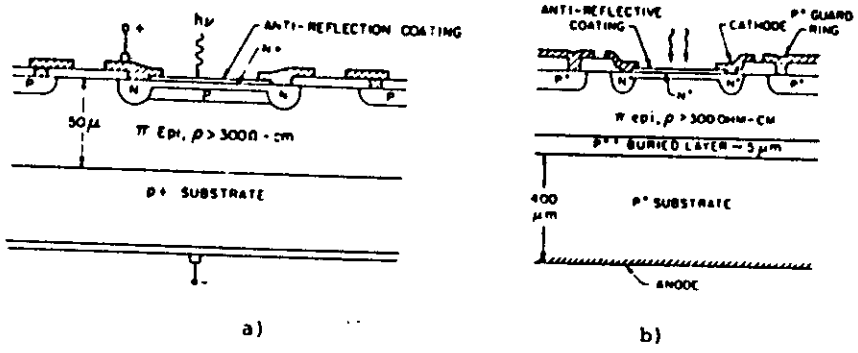

Fig.15 Silicon avalanche photodiodes of the epitaxial n^+-p-π-p^+ type. Light is incident through the high field region in the front and absorbed in the π-region. Electrons initiate the avalanche in the n^+-p high field region. a) High voltage (200-400V) device with thick π region and high (>90%) efficiency and 1 ns speed of response at 0.8-0.9μm /48/.

b) Low voltage type (4-8V) with lower (~60%) efficiency and a speed of response of a few ns /49/.

These reach through structures posses an n^+-p region with a high electric field for carrier multiplication and an extended π region for light absorption and photo-carrier generation.

Reach-through avalanche structures on epitaxial silicon have the advantage of beeing quite compatible with fabrication processes of an integrated-circuit facility.

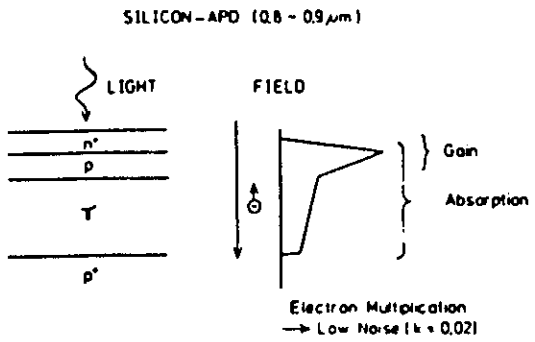

Fig.16 Schematic representation of light absorption and electron multiplication (gain) region of Si n^+-p-π-p^+ avalanche photodiode.

Silicon avalanche photodiodes reach gains in the range of ten to several hundred as illustrated in Fig.16 for the high voltage structure /48/.

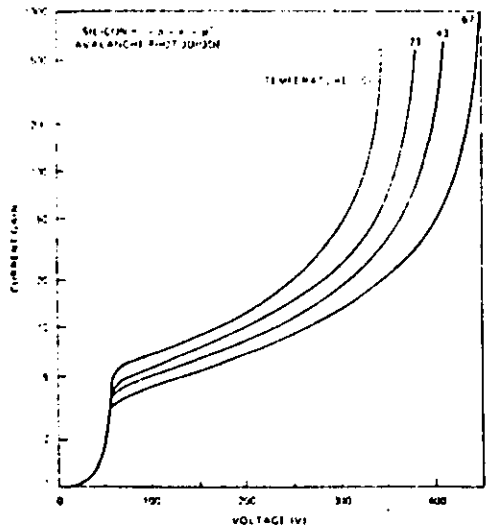

Fig.17 Photomultiplication and current gain characteristics of Si n^+-p-π-p^+ avalanche photodiodes with high efficiency at GaAs laser wavelengths /48/.

In these Si-avalanche photodiodes the excess noise is rather low, at a gain of <M> = 100 the noise factor is only F(100) = 5. As already mentioned, the photoresponse of silicon does not extend much beyond one micrometer. Avalanche photodiodes for longer wavelengths in the 1.2 to 1.6µm range thus have to use other detector-materials.

Germanium photo-and avalanche photodiodes, whose energy gap is narrower are presently used for long-wavelength applications to 1.5 and 1.6µm. While early Ge-APD's /8/ used a mesa construction (see Fig.18a) to suppress dark currents to the 10-30nA range, newer Ge-APD's /9,50,51/ are planar in construction (see Fig.18b) and somewhat more optimized in their electric field profiles.

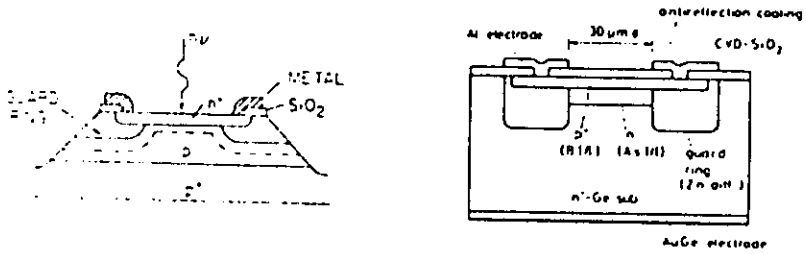

Fig.18 Germanium avalanche photodiodes for the 0.6 to 1.5 wavelength range.
a) Mesa construction /8/, b) Planar type contruction /9,50,51/, both with high quantum efficiency and speed of response of less than 100ps.

These avalanche photodiodes operate in the 10 to 100 Volt range. Since the ionization coefficients of holes are only slightly larger than the ionization coefficients of the electrons the excess noise factor of these diodes increases as

$$F(\langle M\rangle) \geq 1+0.5\ \langle M\rangle \qquad (9)$$

approximately proportional to the current gain. Such avalanche photodiodes are nontheless quite useful to overcome the thermal amplifier noise of the optical receivers and to increase sensitivity.

A basic reason for the investigation of further detector materials and novel avalanche structures /25/ lies in the hope of finding an avalanche photodiode that responds to longer wavelengths in the 1 to 1.6µm range and beyond with avalanche multiplication as low as silicon. Unfortunately none of the III-V detector materials of major interest shows ionization rates with large differences between electrons and holes. In addition, avalanche, photodiodes fabricated in heavily doped narrow gap III-V materials show a tendency for increased dark currents caused by internal field emission /52/.

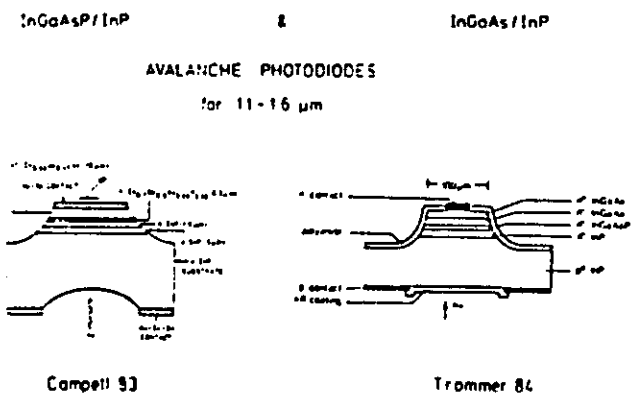

Fig.19 Avalanche photodiodes with light absorbing InGaAsP /15/ and InGaAs /16/ regions for light absorption and n-p InP for carrier multiplication.

The most successful III-V avalanche photodiodes for the 1 to 1.6µm wavelength range thus combine the narrow bandgap material needed for optical absorption with an epitaxially attached material of wider bandgap for carrier multiplication. InGaAs on InP are epitaxially grown avalanche photodiodes of this type /15,16,52-54/.

In InP the holes undergo stronger ionization than the electrons /43/. Low noise avalanche photodiodes have thus been constructed such that the holes initiate the avalanche.

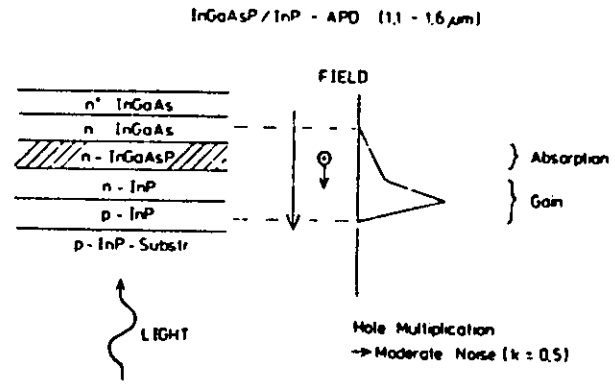

Fig.20 Schematic illustration of p-n-InP-n-InGaAsP-n InGaAs avalanche photodiode structure with light absorption in depleted narrow gap n-InGaAsP region and hole multiplication in n-p InP region.

As the germanium avalanche photodiodes, these InGaAs/InP and InGaAsP/InP photodiodes have reached a state in their development where they offer similar improvements in receiver sensibility in the 1.2 to 1.6µm range as the best fully integrated photodiode receivers. A further search for long wavelength avalanche photodiodes with low noise single carrier multiplication might in the future lead to long wavelength

detectors with properties approaching the best silicon devices.

V. Photodetector Applications including High Sensitivity Receivers

Depending on the needs of a particular application specific types of photodetectors prove most appropriate. A first selection criteria asks for good responsivity or quantum efficiency at the wavelength of operation. For the visible and near infrared to 0.8 and 0.9μm Silicon is the favorite amongst the solid state detector materials. Its technology is far advanced. Detectors, be they simple photodiodes, sophisticated avalanche photodiodes, photoconductors or intricate one or two-dimensional arrays /29,30/, have reached a mature state of development and reliable operation.
Throughout the spectral range where they exhibit high responsivity, they are usually the first choice for most applications, one of the reasons being their low dark currents, often below nanoamperes in the picoampere-range.

Detectors for larger wavelengths in the 1 to 1.6μm region are of necessity chosen from amongst materials with narrower bandgaps, such as Ge, InGaAs, InGaAsP, HgCdTe or the like. With some design effort it is possible to keep the dark circuits of these devices at sufficiently low values to allow room temperature operation even for low light level detection. Detectors for longer wavelengths in the infrared, include HgCdTe /28/, lead salt detectors and III-V compounds like InAs and InSb. To achieve high sensitivity, these detectors usually require cooling.

A further important criteria of detector selection concerns the intensity level of the radiation to be detected. As long as the light intensities to be detected are sufficiently

high, it suffices to consider spectral sensitivity and speed of response of the photodetector. While p-n junction photodiodes and avalanche photodiodes easily reach response times in the nanosecond range, careful device and receiver optimization is necessary to achieve response times in the higher GHz range and below 100 picoseconds.

If weak light levels are to be detected, major attention has to be paid in addition to minimization of noise and leakage circuits in the receiver. As a case in point consider the detection of weak light signals at the end of a digital transmission link. It is a goal of receiver design to provide a signal amplification in the receiver that is as free of excess noise and fluctuation as possible. A light signal of minimal intensity should still be detected with sufficient quality, i.e. a sufficiently high signal-to-noise ratio or low error rate. For digital signal transmission the minimal detectable optical power depends, as indicated in Fig.21, on the quality (quantum efficieny η, avalanche noise F(M)) of the photodetector and the noise $\langle i_{Ampl}^2 \rangle$ within the electrical bandwidth B of the receiver.

DIGITAL TRANSMISSION

Minimal Detectable Power

$$\overline{P_{min}} \geq \frac{h\nu}{e} \frac{Q}{\eta} \left\{ \frac{e\, Q\, B_R\, F(M)}{2} + \frac{\int_0^B \frac{\langle i_{Ampl}^2 \rangle}{\Delta f}\, df}{\sqrt{2}\, R} \right\}$$

no gain (M=1) → amplifier noise $\langle i_{Ampl}^2 \rangle$ dominates

gain (M>1) → Sensitivity increases

Error rate: 10^{-6} Q = 4.8
10^{-9} Q = 6
10^{-12} Q = 7

Fig.21 Minimal detectable power of digital signal reception.

Comparisons of the best reported receivers for fiber optical communication at bit rates from a few Mbit/sec to rates exceeding 1Gbit/sec are illustrated in Fig.22.

While well designed discrete photodiode-FET combinations achieve sensitivities in the -40 to -30dBm range at bit rates between 50 and 500 Mbit/sec considerable improvements in sensitivity are possible with monolithically integrated pin-FET-receivers. This holds for receivers throughout the visible and infrared region to 1.6µm.

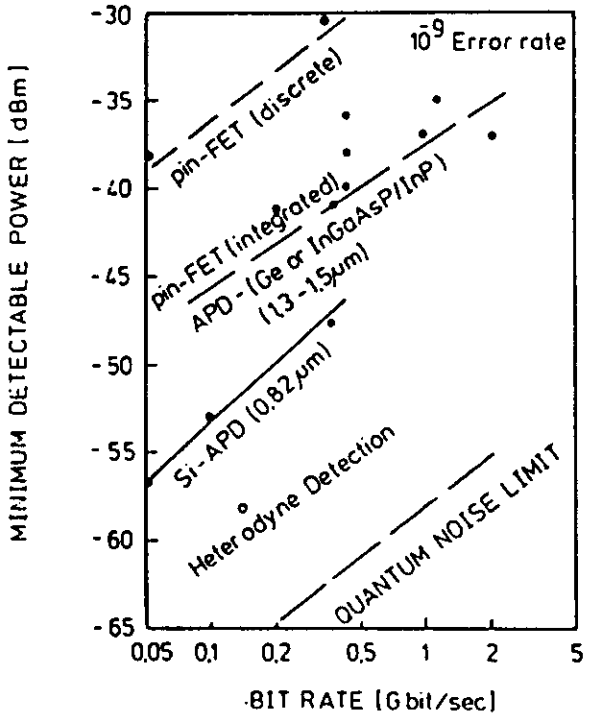

Fig.22 Minimum detectable optical power at input of receivers with photodetectors and low noise amplifier as a function of bit rate for digital signal transmission with an error rate remaining below 10^{-9}.

As illustrated, Si-avalanche photodiodes, due to their "low noise one carrier type multiplication" achieve much higher sensitivities throughout the visible part of the spectrum to about 1µm in the infrared. These sensitivities come to within 10 to 15dB of the best possible ideal quantum noise limited receiver sensitivity.

Germanium, InGaAs/InP and HgCdTe avalanche photodiodes reach high sensitivities in the 1.3 to 1.5µm range. Due to their less than ideal carrier multiplication properties they do not yet fully match the sensitivities of the silicon avalanche diodes. Nontheless it is worthwhile to use avalanche photodiodes, especially at high bit rates. They provide gain up to high speeds since their current gain-bandwidth products easily exceed 100GHz /1,45/.

The development of most of these photodetectors and optical receivers has obtained a major impuls from the needs of fiber-optical communication.

Other important advances are taking place in the development of photodetectors for high speed optoelectronic signal processing and sampling /56-60/.

Interest in this field started when D.Auston /56/ demonstrated that short light pulses from high intensity lasers can serve to activate photoconductive switches and to generate electrical pulses with rise and fall times in the low picosecond range. Initial experiments were done with Si, Ge, CdS and GaAs photoconductive material. A more efficient use of light pulses in the picosecond range has become possible with InP-switches /57/. Such a photoconductive switch is illustrated in Fig.23.

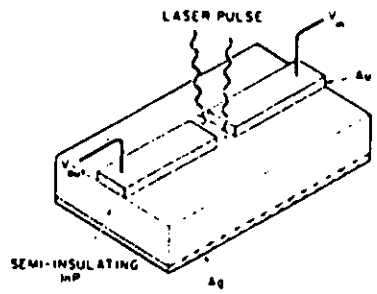

Fig. 23 Indium-Phosphide-photoconductive switch /57/.

This switch is formed by a gap in a microwave strip line on a semiinsulating InP substrate. An incident high intensity laser pulse excites photocarriers in the InP thereby closing the gap between the strip-line electrodes with a highly conducting electron-hole plasma.
The InP is especially treated through ion bombardment such that the photon-excited carriers will recombine within a few picoseconds after cessation of the optical excitation.

A variety of appliacations of these optoelectronic switches are actively beeing explored /59/. As an example Fig.24 shows an application of these high speed switches to the optoelectronic sampling of high speed electronic signals /59/. In this case, photoconductive sampler is actually used to measure the pulse response of a high speed silicon photodiode /24/. While a sequence of weak light pulses is incident on the photodiode, stronger light pulses with subsequently later arrival times serve to activate the photoconductive sampler.

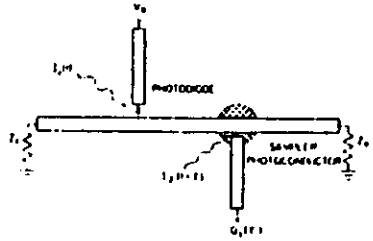

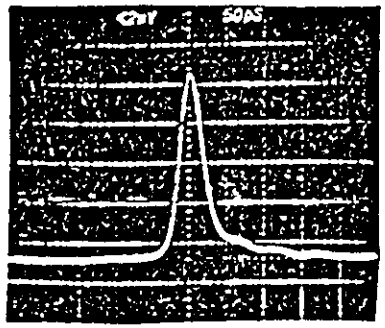

Fig.24 Picosecond optoelectronic sampling (Photoconductive switch samples signal of high speed photodiode)/56,59/.

A further experiment /60/ illustrates the use of a pulsed semiconductor laser to achivate a photoconductive sampling gate made from semiinsulating GaAs of a few micrometers in dimension. (Fig.25).

These types of photoconductive switches offer a number of interesting possibilities for application in optical and optoelectronic signal processing in hybrid and eventually in fully integrated optics.

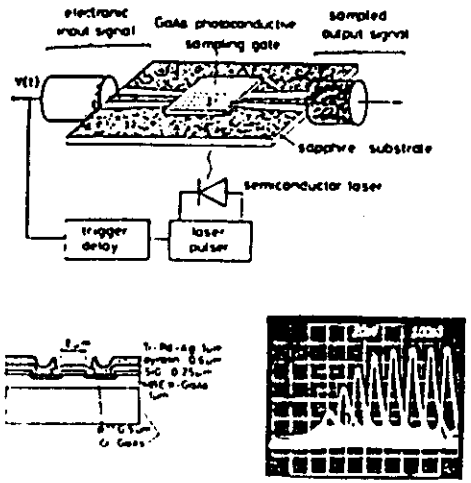

Fig.25 Optoelectronic sampler combining pulsed semiconductor laser with high-speed photoconductive GaAs-gate of a few micrometer in dimension on a tapered coplanar mounting structure. The switch consists of Cr doped GaAs. Up to the present time resolutions of order 50 picoseconds have been achieved as illustrated by the sequence of sampling pulses in the bottom part of the figure. /60/.

As mentioned, a number of well developed and highly perfected photodetectors are available for application in integrated optics throughout the visible and infrared part of the spectrum. Most of these detectors come in the form of single, discrete devices. Amongst the photodiodes one and two dimensional arrays are available. In addition the first fully electronically integrated detector-receiver combinations begin to appear. In most cases these detectors are placed and mounted at the outputs of integrated optics arrangements. Their size is usually sufficiently large that easy placement is possible. Hybrid arrangements allow the detectors and electronic receivers to be optimized separaltly from the integrated optics. Fully monolithically optic- and electronically integrated arrangements are a rarity at this time. The development of integrated optics will however undoubtedly bring fully optically and electronically integrated detectors and receivers, at least for specific applications where large members of receivers warrant their development.

References:

1. H.Melchior, in Laser-Handbook, edited by F.T.Arecchi and E.O.Schulz-Dubois, North Holland, New York 1972.

2. P.W.Kruse, L.D.McGlauchlin and R.B.McQuistan , Infrared Technology, John Wiley, New York 1962.

3. H.Melchior, in Physics and Technology of Semiconductor Light Emitters and Detectors, edited by A.Frova, North Holland, New York 1973 und J.Luminescence, vol.7, pp.390-414, 1973.

4. G.E.Stillman and C.M.Wolfe, in Semiconductors and Semimetals, vol.2, Infrared Detectors II, edited by R.K.Willandson and A.C.Beer, Academic Press, New York 1977.

5. T.P.Lee and T.Li, in Optical Fiber Communications, edited by S.E.Miller and A.G.Chynoweth, Academic Press, New York, 1979.

6. R.G.Smith, Proc.IEEE, vol.68, pp.1247-1253, Oct.1980.

7. Y.Suematsu, Proc.IEEE, vol.71, pp.692-721, Juni 1983.

8. H.Melchior and W.T.Lynch, IEEE Trans. on Electron Devices, vol.13, pp.829-838, Dec.1966.

9. T.Mikawa, S.Kagawa, T.Kaneda, T.Sakurai, H.Ando and O.Mikami, IEEE J.Quantum Electronics, QE-17, pp.210-216, Febr.1981 and El.Lett. vol.19, pp.452-453, Juni 1983.

10. C.E.Hurwitz and J.J.Hsich, Appl.Phys.Lett. vol.32, pp.487-489, Apr.1978.

11. T.P.Pearsall and M.Papuchon, Appl.Phys.Lett. vol.33, pp.640-642, Oct.1978.

12. R.F.Leheny, R.E.Wahonz and M.A.Pollack, El.Lett.vol.15, pp.713-715, Oct.1979.

13. H.Kanbe, N.Susa, H.Nakagome and H.Ando, El.Lett.vol.16, pp.163-165, Febr.1980.

14. T.P.Lee, C.A.Burrus and A.G.Dentai, IEEE J.Quantum-Electron. QE-17, pp.232-238, Febr.1981.

15. J.C.Campbell, A.G.Dentai, W.S.Halden and B.L.Kasper, El.Lett.vol.9, pp.818-820, Sept.1983.

16. R.Trommer, Proc.9th Europ.Conf.on Opt.Comm. edited by H.Melchior and A.Sollberger, pp.159-162, North Holland, Amsterdam, 1983.

17. M.Kobayashi, S.Yamazakipand, T.Kaneda, Appl.Phys.Lett. vol.45, pp.759-761, Oct.1984.

18. K.Ogawa and E.L.Chinnock, El.Lett. vol.55, pp.650-652, Sept.1979.

19. R.Leheny, R.Nahory, M.Pollack, A.Ballmann, E.Beebe, J.De Winter and R.Martin, El.Lett.vol.16, pp.353-355, Mai 1980.

20. M.C.Brain, P.P.Smith, D.R.Schmith, B.R.White and P.S.Chidgey, El.Lett., vol.20, pp.894-896, Oct.1984.

21. T.Nakagami, M.Sasaki and T.Sakurai, Opt.Fiber Comm. Conf., San Diego US. pp.32-33, Febr.1985.

22. D.B.Ostrowsky, R.Poirier, L.M.Reiben and C.Deverdem, Appl.Phys.Lett. vol.22, pp.463-ff, 1973.

23. T.van Muoi, IEEE J.Lightwave Techn. LT-2, pp.243-267, June 1984.

24. H.Melchior, Physics Today, vol.30, pp.32-39, Nov.1977.

25. F.Capasso and W.T.Tsang, ATT Bell Lab.Recond, pp.13-19, March 1984.

26. T.Okoshi, 7th Optical Fiber Comm.Conf., pp.60-61, New Orleans, Jan.1984.

27. T.G.Hodgkinson, D.W.Smith, R.Wyatt and D.J.Malyon, 8th Optical Fiber Comm.Conf., pp.22-23, San Diego, Febr.1985.

28. M.Roger and C.Vené, 7th Europ.Conf.on Opt.Comm. Copenhagen, Sept.1981.

29. C.H.Seguin and M.F.Tompsett, Charge Transfer Devices, Academic Press, New York, 1975.

30. L.J.M.Esser and F.L.J.Sangster in Handbook of semiconductors, vol.4, pp.335-424, edited by T.S.Moss and C.Hilsum, North Holland, Amsterdam 1981.

31. S.Y.Wang, D.M.Bloom, El.Lett.vol.19, pp.554-555, July 1983.

32. J.Goell, Bell.Syst.Techn.J.vol.53, pp.629-643, April 1974.

33. R.G.Smith, C.A.Brachett and H.W.Reinbold, Bell.Syst.Techn. J. vol.67, pp.1809-1822, July 1978.

34. R.C.Hooper, H.A.Z.Rejman, S.T.D.Richie, D.R.Smith and B.R.White, Proc.6th Europ.Conf.Opt.Comm. York, pp.222-225, 1980.

35. M.G.Brown, S.R.Forrest, P.Hu, D.R.Kaplan, M.Koza, Proc.Int.El.Device Metting, p.727-728, San Franzisco, Dec.1984.

36. L.Mandel, Proc.Phys.Soc.vol.74, pp.233ff, 1959.

37. D.E.McCumber, Phys.Rev. vol.141, pp.306, 1966.

38. H.Melchior, H.Jaeckel and R.Welter in Integrated Optics ed.by S.Martellucci and A.N.Chester, Plenum Press, New York, 1983.

39. O.Wasa, S.Miura, M.Ito, T.Fujii, T.Sakurai and S.Hiyamizu, Appl.Phys.Lett. vol.42, 380, 1983.

40. R.M.Kolbas, J.Abrokwah, J.K.Carney, D.H.Bradshaw, B.R.Elmer and J.R.Biard, Appl.Phys.Lett. vol.43, pp.821-823, Nov.1983.

41. T.Nakagami, M.Sasaki and T.Sakurai, Proc.8th Conf.Opt. Fiber Comm. San Diego, pp.32-33, Febr.1985.

42. S.Sze, Physics of Semiconductor Devices, p.47, John Wiley, New York 1981.

43. C.A.Armiento and S.H.Groves, Appl.Phys. Lett., vol.43, pp 198-200, July 1983.

44. R.J.McIntyre, IEEE Trans.of Electron Devices, ED-13, pp.164-168, Jan.1966.

45. B.Emmous, J.Appl.Physl.vol.38, pp.3705-3714, Aug.1967.

46. H.Ruegg, IEEE Trans.Electron-Devices, ED-14, pp.239-251, May 1967.

47. R.P.Webb, R.J.McIntyre and J.Conradi, RCA Rev. vol.35, p.234, 1974.

48. H.Melchior, A.R.Hartmann, D.P.Schicke and T.E.Seidel, Bell System Techn.Journal, vol.57, pp.1791-1807, July 1978.

49. G.K.Chang, A.R.Hartmann, M.Robinson, T.J.Riley and R.Y.Lee, Proc.Int.Electron Devices Meeting, pp.733-736, San Franzisco, Dec.1984.

50. H.Ando, H.Kaube, T.Kumura, T.Yamaoka and T.Kaneda, IEEE J. Quantum Electron. QE-14, pp.804-809, Nov.1978.

51. M.Niwa, Y.Tashiro, K.Minemuray and H.Iwasaki, Electron. Lett. vol.20, pp.552-553, 1984.

52. S.R.Forrest, O,K.Kimpand, R.G.Smith, Appl.Phys.Lett. vol.41, pp.95-99, 1982.

53. K.Taguchi, Y.Matsumoko and K.Nishida, Electr.Lett. vol.15, pp.453-455, 1979.

54. M.Kanbe, N.Sura, H.Nakagome and H.Ando, Electron.Lett. vol.16, pp.155-156, 1980.

55. Y.Sugimoto, T.Torikai, K.Makita, H.Ishikana, K.Minemura, K.Taguchi and T.Iwakami, Electron.Lett. vol.20, pp.653-654, Aug.1984.

56. D.H.Auston, Appl.Phys.Lett. vol.26, pp.101-103, 1975.

57. F.J.Leonberger and P.F.Moulton, Appl.Phys.Lett. vol.35, pp.712-714, 1979.

58. D.H.Anston and P.R.Smith, Appl.Phys.Lett. vol.47, pp 599-601, Oct.1982.

59. C.H.Lee, Picosecond Optoelectronic Devices, Academic Press, New York, 1984.

60. P.Schmid and H.Melchior, Electron.Lett. vol.20, pp.684-685, Aug.1984.